Available online at www.sciencedirect.com
SCIENCE DIRECT
Bioorganic & Medicinal Chemistry Letters
Bioorganic & Medicinal Chemistry Letters 16 (2006) 4053–4058

Identification of metabolites of the tryptase inhibitor CRA-9249: Observation of a metabolite derived from an unexpected hydroxylation pathway

Walter Yu,[a] Jeffrey M. Dener,[c,*] Daniel A. Dickman,[c] Paul Grothaus,[b] Yun Ling,[a] Liang Liu,[a] Chris Havel,[a] Kimberly Malesky,[b] Tania Mahajan,[b] Colin O'Brian,[c] Emma J. Shelton,[b] David Sperandio,[b] Zhiwei Tong,[b] Robert Yee[b] and Joyce J. Mordenti[a]

[a]*Department of Drug Metabolism and Pharmacokinetics, Celera Genomics, 180 Kimball Way, South San Francisco, CA 94080, USA*
[b]*Department of Medicinal Chemistry, Celera Genomics, 180 Kimball Way, South San Francisco, CA 94080, USA*
[c]*Department of Process Chemistry, Celera Genomics, 180 Kimball Way, South San Francisco, CA 94080, USA*

Received 24 February 2006; revised 28 April 2006; accepted 1 May 2006
Available online 18 May 2006

Abstract—The metabolites of the tryptase inhibitor CRA-9249 were identified after exposure to liver microsomes. CRA-9249 was found to be degraded rapidly in liver microsomes from rabbit, dog, cynomolgus monkey, and human, and less rapidly in microsomes from rat. The key metabolites included cleavage of an aryl ether, in addition to an unexpected hydroxylation of the amide side chain adjacent to the amide nitrogen. The chemical structures of both metabolites were confirmed by synthesis and comparison to material isolated from the liver microsomes. Several suspected hydroxylated metabolites were also synthesized and analyzed as part of the structure identification process.

Metabolite identification is a critical step in the development of new chemical entities (NCEs).[1] Understanding the metabolic fate of potential therapeutic agents early in the drug discovery process helps to identify those compounds that may be rapidly metabolized and excreted before they can exert their pharmacological benefit in vivo.[2] This understanding is particularly important before the development of the active pharmaceutical ingredient (API) and the initiation of the more expensive and time consuming preclinical studies, such as GLP toxicology studies. Increasingly, an integrated effort between medicinal chemistry, drug metabolism, and toxicology departments to understand the metabolic liabilities and toxicological profile of the lead candidate will provide direction to identify and develop a clinical candidate with an improved metabolic profile. Typically, this approach incorporates an iterative design effort through the use of in vitro predictors of metabolic liabilities. In fact, several recent reports have highlighted the successful application of iteration in identifying metabolites that have a better pharmacological profile than the lead drug candidate. The best example of a marketed product to come from a metabolite-driven drug development program is the cholesterol absorption inhibitor, Zetia® (Ezetimibe; SCH 58235).[3] While the identification of an active metabolite may be beneficial to a drug development program, some active metabolites can induce adverse effects in vivo,[4] and appropriate testing is required to assess this possibility.

Celera has developed a novel series of bis(benzimidazole)methane-containing tryptase inhibitors as potential agents for allergic and inflammatory diseases, in particular asthma.[5] One such derivative is the bis(benzimidazole) difluoromethane inhibitor CRA-9249 (**1**) (Scheme 1), an orally bioavailable inhibitor of mast cell tryptase. During our preclinical development program for CRA-9249 for the treatment of asthma, we studied its metabolism in vitro to identify its metabolic profile and stability, and to predict its metabolic fate in vivo.

Exposure of CRA-9249 to an aqueous suspension of homogenized liver microsomes from four species [mouse, dog, cynomolgus (cyno) monkey, and human]

Keywords: Metabolism; Metabolite identification; Synthesis; Active metabolite.
* Corresponding author. Tel.: +1 650 866 6695; fax: +1 650 866 6655; e-mail: jdener@yahoo.com

0960-894X/$ - see front matter © 2006 Elsevier Ltd. All rights reserved.
doi:10.1016/j.bmcl.2006.05.003

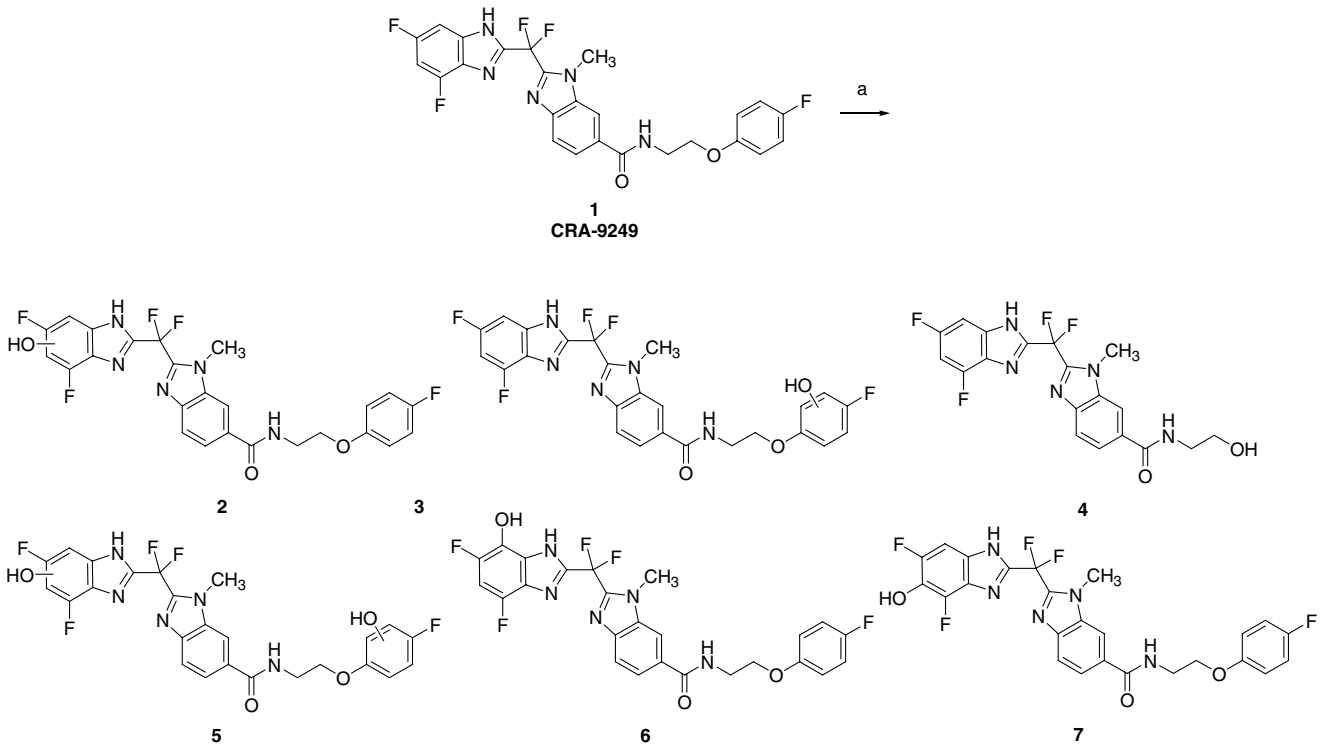

Scheme 1. Metabolism of the tryptase inhibitor CRA-9249 (**1**). Reagents and conditions: (a) 20 μM CRA-9249, liver microsomes (1.5 mg protein/mL) from five species, 2 mM NAPDH, 10 mM $MgCl_2$, 37 °C, up to 3 h.

resulted in rapid degradation of the parent and formation of several metabolites. In these species, less than 10% of the parent drug was detected after a 3-h exposure period. However, metabolism of **1** in rat liver microsomes was much slower, with 56% of the parent remaining after exposure over the same 3-h period. Employing LC/MS/MS analysis, a total of five Phase 1 metabolites were identified from these in vitro liver microsome incubation experiments. Furthermore, the relative rate of disappearance of the parent **1** was species dependent, according to the order of cyno monkey > rabbit > dog > human ≫ rat.

Monohydroxylation and O-dearylation were the two predominant metabolites produced from **1** after exposure to liver microsomes from all five species, although the rate of formation of the monohydroxylated metabolite was different depending on the species. To better understand the fate of **1**, we initiated a program to synthesize several of the proposed structures to confirm the structural identity of each of the major metabolites. In addition, we evaluated the in vitro potency (K_i) of these synthetic samples in Celera's zinc-dependent tryptase assay to determine if any of these could be active metabolites of the parent compound CRA-9249. As shown in Scheme 1, these metabolites included monohydroxylation, dihydroxylation, and dearylation. Based on these LC/MS/MS studies, generic structures **2** and **3** were considered the most plausible structures for the monohydroxylated metabolite. The hydroxyethylamide **4** was proposed as the dearylated metabolite. Finally, generic structure **5** was proposed for the minor dihydroxylated metabolite. Our initial target structures for synthesis included the O-dealkylation product **4** and aromatic hydroxylation derivatives **6** and **7**. Finally, a large-scale incubation of CRA-9249 in cyno monkey liver microsomes was performed to assist in the confirmation of the identity of these metabolites, allowing for the generation of proton-, carbon-, and fluorine-NMR data from the metabolite mixture. Synthesis of the O-dearylated species (**4**) was accomplished in one step by the reaction of the acid **8**[6] with PyBroP and 500 mole percent of ethanolamine in DMF as shown in Scheme 2. O-dearylated metabolite **4** was obtained after aqueous work-up and crystallization.

The synthesis of proposed 4- and 6-hydroxybenzimidazole derivatives **6** and **7** proved to be more challenging. The synthesis of **6** started from commercially available 2,4,5-trifluoroaniline (**9**) (Scheme 3), which was acetylated and nitrated according to a literature procedure to give nitro derivative **11**.[7] Heating **11** with aqueous sodium hydroxide resulted in displacement of the fluorine adjacent to the nitro group, as well as deacetylation of the aniline. The crude product was not isolated but

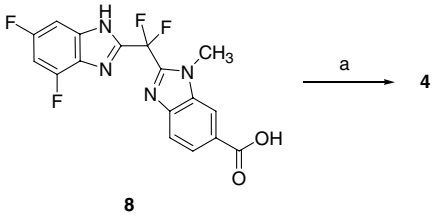

Scheme 2. Reagents and conditions: (a) PyBroP, 2-aminoethanol (500 mole %), DMF then crystallization, 31%.

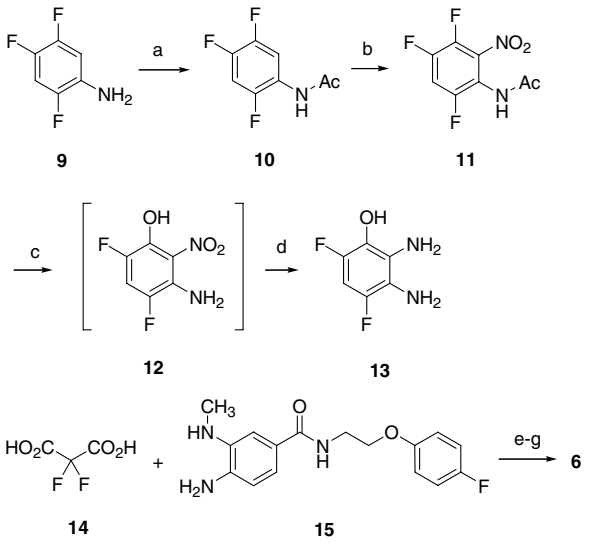

Scheme 3. Reagents and conditions: (a) Et_3N, THF, RT to −20 °C then AcCl, <20 °C, 90%; (b) 25% AcOH in H_2SO_4 then HNO_3/H_2SO_4/AcOH (4:1:1), 50%; (c) aq NaOH, 85 °C to reflux; (d) H_2, 10% Pd–C, EtOH, 48% from **11**; (e) PyBroP, *N*-methylmorpholine (NMM), DMF, −10 °C; (f) PyBrOP, DMF, −10 °C, then **13**, NMM. −10 °C; (g) AcOH, 85 °C, 9% from **15**.

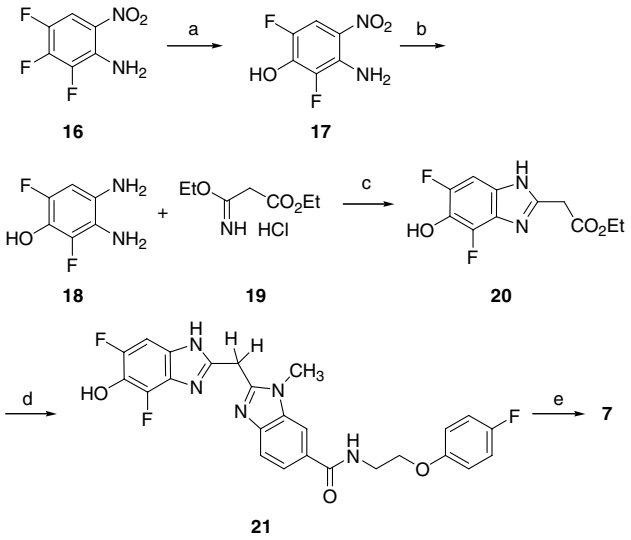

Scheme 4. Reagents and conditions: (a) aq NaOH, DMPU, 120 °C, 86%; (b), H_2, 10% Pd–C, EtOH; (c) **19**, EtOH, reflux, 43% from **17**; (d) **15**, DMPU, 185 °C, 73%; (e) $(PhSO_2)_2N$–F, EtOH, reflux, 3%.

converted directly to **13** by catalytic reduction of the nitro group. The formation of the bis(benzimidazole)difluoromethane fragment was accomplished in a one-pot reaction consisting of four chemical transformations.[8] 2,2-Difluoromalonic acid (**14**) was treated with PyBroP and *N*-methylmorpholine (NMM) in DMF, then by 4-amino-3-(methylamino)benzamide **15** was added. Another equivalent of PyBroP was added, followed by diamine **13** and another portion of NMM. Finally, the mixture was worked up and the crude product was heated in acetic acid to give the desired putative metabolite **6** after chromatographic purification.

Synthesis of putative metabolite **7** was accomplished as described in Scheme 4. Commercially available 2,3,4-trifluoro-6-nitroaniline (**16**) was reacted with aqueous sodium hydroxide to introduce the required hydroxyl functionality at C-3. The nitro group in **17** was reduced to the 1,2-diaminobenzene **18**, which was converted to the corresponding 4,6-difluoro-5-hydroxybenzimidazole **20** by heating with imidate **19** in ethanol. Condensation of the ester in **20** with diamine **15** in DMPU at 185 °C afforded the bis(benzimidazole)methane derivative **21**. Fluorination of the bridgehead methylene of **21** was accomplished with *N*-fluorobenzenesulfonylimide to provide the desired 6-hydroxybenzimidazole derivative **7**.[9]

Analysis of DMSO–water solutions obtained from the liver microsome incubation of **1** confirmed the presence of compound **4** by HP LC–UV and LC–MS analysis and comparison of these data with the authentic sample of **4** prepared as described above.[10] However, the presence of **6** or **7** could not be confirmed in the metabolite mixture. Analysis of the metabolite broth from the large-scale microsome incubation study by ^{19}F NMR did not provide a match to the fluorine NMR of synthetic compound **7**.

However, a clue to the structural identity of the probable mono-hydroxylated species arose from identification of a secondary metabolite, the primary amide **22**, which was identified by LC–MS analysis of the metabolite broth when it was reanalyzed about one month after incubation (Scheme 5). Subsequently, the presence of **22** in the microsome incubation broth was confirmed by HPLC analysis by co-injection of a mixture of an authentic sample of **22** with the metabolite broth. From this observation, hydroxylation at the α-methylene carbon of the amide nitrogen of **1** (compound **23**) was proposed as a potentially unstable metabolite, which could undergo hydrolysis to give amide **22** and the 2-(4-fluorophenoxy)acetaldehyde (**24**) upon standing in the aqueous medium from the liver microsome incubations.

N-dealkylation of secondary and tertiary amides via metabolic pathways is well documented in the literature and presumably occurs via hydrolysis of the unstable α-hydroxyamide; however, literature reports of the isolation and characterization of these α-hydroxyamide metabolites are limited due to this propensity to undergo hydrolysis to the amide and aldehyde.[11] An early example of α-hydroxylation of an amide was reported for an anticonvulsant oxadiazole, containing an *N*-methyl-*N*-acetamide moiety, which underwent hydroxylation at the *N*-methyl group, as well as hydrolysis to the secondary amide.[12] Furthermore, *N*,*N*-dimethylbenzamides have been shown to provide *N*-(hydroxymethyl)-*N*-methylbenzamides in liver microsomes.[13] A more relevant example is the metabolism of the anti-diabetic agent glyburide (**25**) (Scheme 6), which contains some structural similarity to **1**.[14] Glyburide also undergoes α-hydroxylation to the hydroxyamide **26**, in addition to hydroxylation adjacent to the benzene ring (**27**) and hydroxylation at various positions on the cyclohexyl ring.

In order to provide experimental evidence to support the α-hydroxylation of **1**, the synthesis of proposed

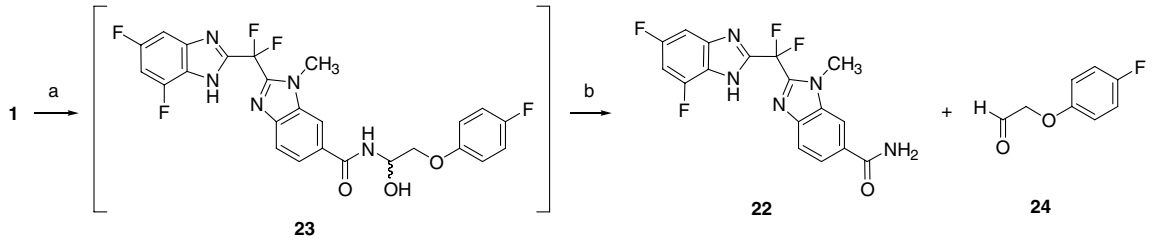

Scheme 5. Proposed pathway for the formation and degradation of the α-hydroxyamide metabolite **23**. (a) 20 μM CRA-9249, liver microsomes (1.5 mg protein/mL) from five species, 2 mM NAPDH, 10 mM $MgCl_2$, 37 °C, up to 3 h; (b) DMSO–water, ~1 month.

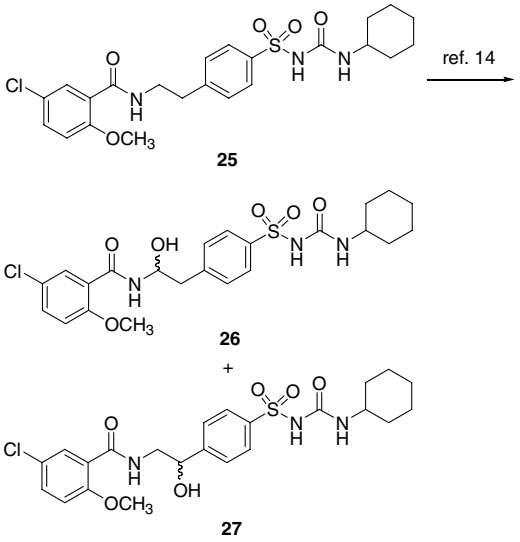

Scheme 6. Metabolites of glyburide (**25**).

metabolite **23** was performed according to Scheme 7, the key step of which is essentially the reverse of the metabolite degradation process. Reaction of acid **8** with ammonia and PyBrOP afforded the primary amide component. Synthesis of the aldehyde fragment **24** was accomplished by alkylation of 4-fluorophenol (**28**) with bromoacetaldehyde dimethoxy acetal to give the protected aldehyde, which was hydrolyzed directly to the aldehyde **24** with a catalytic quantity of sulfuric acid in aqueous acetic acid.[15] Reaction of amide **22** with this aldehyde in refluxing acetonitrile afforded the desired α-hydroxybenzamide **23** in low yield but in sufficient quantity for isolation and characterization of a small sample. The corresponding dehydration product, the *N*-acylimine **29**, was also produced in trace amounts in the reaction.[16] Compound **23** was unstable on standing and was determined by LC–MS analysis to degrade back to **22** and **24**. The synthetic material corresponding to proposed structure **23** was shown to be identical to the major metabolite of CRA-9249 (**1**) upon analysis of this mixture based on HPLC retention time, mass spectral fragmentation, and parent ions. Furthermore, proton NMR of the synthetic material provided a match of the major signals for the proton NMR spectrum that were obtained from the large-scale metabolite incubation study.[17–19]

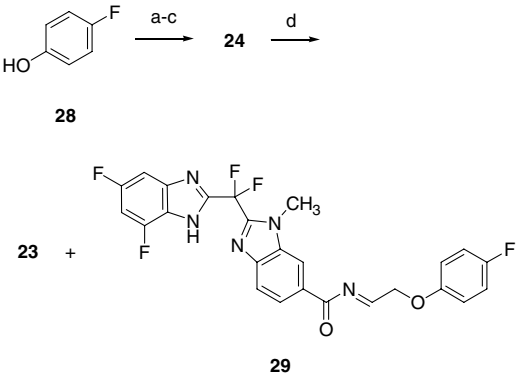

Scheme 7. Reagents and conditions: (a) 1 M *t*-BuOK in THF, DMSO; (b) $BrCH_2CH(OCH_3)_2$; (c) H_2SO_4 (cat), acetone–water (10:1), 33% from **28**; (d) **22**, CH_3CN, 90 °C, 3% after preparative HPLC.

Finally, we determined the equilibrium constants for binding of synthetic metabolite derivatives **4**, **6**, **7**, and **23** to tryptase. Apparent inhibition constants (K_i) for these compounds were determined using Celera's zinc-dependent tryptase assay as described previously.[5] Data for these metabolites, as well as the parent compound CRA-9249 (**1**), are shown in Table 1.

As shown in Table 1, the O-dearylated metabolite **4** and the synthetic aryl monohydroxy metabolite **7** possessed low micromolar activity against tryptase and were 4- and 23-fold less active than the parent in the enzyme assay; interestingly, however, both the synthetic aryl monohydroxylated derivative **6** and the major metabolite, α-hydroxyamide **23**, were 8.8 and 12.5 times more potent than the parent compound **1**.

Although the increased potency of **6** could be a result of participation by the aryl hydroxy group in the zinc-mediated binding of the compound at the active site of tryptase,[5] the increased potency of α-hydroxyamide **23** is not so clear. However, one possible explanation is that **23** is converted to *N*-acylimine **29** which then irreversibly binds to the enzyme.[20] In any event, due to the rapid

Table 1. In vitro inhibition of mast cell tryptase by compound **1** and synthetic samples of proposed metabolites

Compound	K_i (μM)
1	0.3
4	7.0
6	0.034
7	1.4
23	0.024

metabolism of **1** in human liver microsomes and the instability of the major metabolite **23**, compound **1** was not considered as a viable candidate for continued development.[21]

Acknowledgments

We thank Drs. Mike Green and Mike Venuti for their support, guidance, and commitment during the execution of this work.

References and notes

1. (1) Yan, Z.; Caldwell, G. W. *Curr. Topics Med. Chem.* **2001**, *1*, 403; (2) Elkins, S.; Ring, B. J.; Grace, J.; McRobie-Belle, D. J.; Wrighton, S. A. *J. Pharmacol. Toxicol. Methods* **2000**, *44*, 313.
2. Fura, A.; Shu, Y.-Z.; Zhu, M.; Hanson, R. L.; Roongta, V.; Humphreys, W. G. *J. Med. Chem.* **2004**, *47*, 4339.
3. (a) Rosenblum, S. B.; Huynh, T.; Alfonso, A.; Davis, H. R., Jr.; Yumibe, N.; Clader, J. W.; Burnett, D. A. *J. Med. Chem.* **1998**, *41*, 973; (b) Clader, J. W. *J. Med. Chem.* **2001**, *47*, 1.
4. (a) Piromohamed, M.; Kitteringham, N. R.; Park, B. K. *Drug Safety* **1994**, *11*, 114; (b) Williams, D. P.; Naisbitt, D. J. *Curr. Opin. Drug Disc. Dev.* **2002**, *5*, 104; (c) Nassar, A.-E. F.; DeMaio, W.; Davis, M.; Talaat, R. E. *Curr. Drug Disc.* **2004**, 20.
5. (a) Janc, J. W.; Clark, J. M.; Warne, R. L.; Katz, B. A.; Moore, W. R. *Biochemistry* **2000**, *39*, 4792; (b) Katz, B. A.; Clark, J. M.; Finer-Moore, J. S.; Jenkins, T. E.; Johnson, C. R.; Ross, M. J.; Luong, C.; Moore, W. R.; Stroud, R. M. *Nature* **1998**, *391*, 608; (c) Church, T. J.; Cutshall, N. S.; Gangloff, A. R.; Jenkins, T. E.; Linsell, M. S.; Litvak, J.; Rice, K. D.; Spencer, J. R.; Wang, V. R. PCT Int. Appl. WO 9845275, 1998.
6. Dener, J. M.; O'Bryan, C.; Yee, R.; Shelton, E. J.; Sperandio, D.; Mahajan, T.; Palmer, J.; Spencer, J. R.; Tong. Z. *Tetrahedron Letters*, accepted for publication.;
7. Finger, G. C.; Reed, F. H.; Burness, D. M.; Fort, D. M.; Blough, R. R. *J. Am. Chem. Soc.* **1951**, *73*, 145.
8. Mittendorf, J.; Henning, R.; Raddatz, S.; Schlemmer, K.-H.; Hiraoka, M.; Kadono, H.; Mogi, M.; Moriwaki, T.; Murata, T.; Sakakibara, S.; Shimada,.M.; Yoshida, N.; Yoshino. T. PCT Int. Appl. WO 0020401, 2000. The sequence presumably goes through the monoamide and bis(amide) intermediates **A** and **B**. Yields of this process tended to be low due to the formation of symmetrical bis(amide) derivatives from two molecules of **14** with reaction **15**.

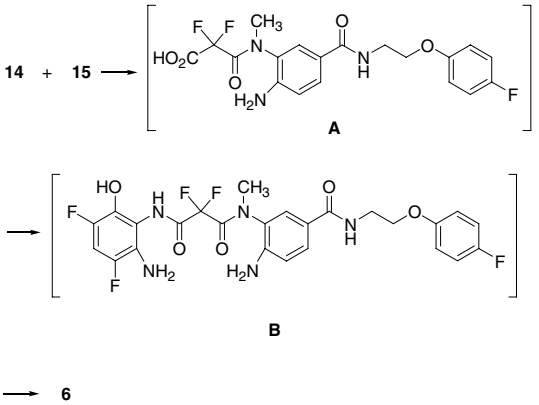

9. Sperandio, D.; Gangloff, A. R.; Litvak, J.; Goldsmith, R.; Hataye, J. M.; Wang, V. R.; Shelton, E. J.; Elrod, K.; Janc, J. W.; Clark, J. M.; Rice, K.; Weinheimer, S.; Yeung, K.-S.; Meanwell, N. A.; Hernandez, D.; Staab, A. J.; Venables, B. L.; Spencer, J. S. *Bioorg. Med. Chem. Lett.* **2002**, *12*, 3129.
10. Positive and negative ion mass spectral data for metabolite **4** are as follows: $m/z = 422.2$ $[M+H]^+$; $m/z = 420.3$ $[M-H]^-$. The synthetic sample of **4** provided the following data: $m/z = 422.1$ $[M+H]^+$; $m/z = 420.2$ $[M-H]^-$.
11. For representative examples of metabolism-mediated N-dealkylation of amides in vitro and in vivo, please see the following references: (a) Sugnaux, F. R.; Benakis, A. *Eur. J. Drug Metab. Pharmacokinet.* **1978**, *3*, 235; (b) Yoshida, K.; Manbu, K.; Arakawa, S.; Miyazaki, H.; Hashimoto, M. *Biomed. Mass Spectrom.* **1979**, *6*, 253; (c) Schoenig, G. P., ; Hartnagel, R. E., Jr.; Osimitz, T. G.; Llanso, S. *Drug. Metab. Dispos.* **1996**, *24*, 156; (d) Constantino, L.; Iley, J. *Xenobiotica* **1999**, *29*, 409.
12. Allen, J. G.; Blackburn, M. J.; Caldwell, S. M. *Xenobiotica* **1971**, *1*, 3–12.
13. Ross, D.; Farmer, P. B.; Geschner, A.; Hickman, J. A.; Threadgill, M. D. *Biochem. Pharmacol.* **1983**, *32*, 1773.
14. Tiller, P. R.; Land, A. P.; Jardine, I.; Murphy, D. M.; Sozio, R.; Ayrton, A.; Schaefer, W. H. *J. Chromatogr. A* **1998**, *794*, 15.
15. Smith, R. L.; Bicking, J. B.; Gould, N. P.; Lee, T.-J.; Robb, C. M.; Keuhl, F. A., Jr.; Mandel, L. R.; Cragoe, E. J., Jr. *J. Med. Chem* **1977**, *20*, 540.
16. The presence of imine **29** in this reaction was proposed based on LC–MS data from the crude product obtained from the synthesis of **23**. Only a few reports of *N*-acylimines derived from aliphatic aldehydes are represented in the literature since these are known to isomerize to the corresponding enamide: Gizecki, P.; Dhal, R.; Poulard, C.; Gosselin, P.; Dujardin, G. *J. Org. Chem.* **2003**, *68*, 4338. Imine **29** may also be produced during the metabolism of **1** in liver microsomes, but it is expected to readily hydrolyze to **22** and **24** under the aqueous conditions employed (see also Ref. 19).
17. The analytical data for the synthetic sample of metabolite **23** are as follows: ^{1}H NMR (DMSO-d_6; 500 MHz) δ 8.97 (d, 1H, CONH), 8.29 (s, 1H, ArH), 8.18 (s, 1H, NH) 7.88 (dd, 1H, ArH), 7.79 (d, 1H, ArH), 7.08–7.15 (m, 2H, ArH), 6.97–7.03 (m, 2H, ArH), 6.83 (br s, 2H, ArH), 6.32 (d, 1H, OH), 5.75–5.81 (m, 1H, OCHN), 4.07 (dt, 2H, NCH_2), 3.87 (s, 3H, CH_3); LC–MS: m/z 532.2 $[M+H]^+$, 377.9 $[M-154]^+$. The mass-to-charge ratio of 377.9 corresponds to the ion for the protonated ($[M+H]^+$) primary amide **22**. For comparison, compound **1** provided the following analytical data: ^{1}H NMR (DMSO-d_6; 500 MHz) δ 8.82 (t, 1H, CONH), 8.31 (s, 1H, ArH), 7.85 (dd, 1H), 7.78 (d, 1H, ArH), 7.33 (d, 1H, ArH), 7.23 (br t, 1H, ArH), 7.14–7.08 (m, 2H, ArH), 7.01–6.96 (m, 2H, ArH), 4.12 (t, 2H, OCH_2), 4.02 (s, 3H, CH_3), 3.67 (q, 2H, NCH_2); LC–MS: m/z 516.1 $[M+H]^+$, 538.0 $[M+Na]^+$.
18. The metabolite broth provided a proton NMR spectrum that contained the following signals in common with the proton spectrum for synthetic **23**: ^{1}H NMR (DMSO-d_6; 500 MHz) δ 9.01 (d, CONH), 8.36 (s, ArH), 7.89 (d ArH), 7.80 (d, ArH), 7.08–7.14 (m, ArH), 6.96–7.03 (m, ArH), 6.83 (br s, 1H, ArH), 6.32 (d, OH), 5.74–5.82 (m, OCHN), 4.07 (dt, NCH_2), 4.03 (s, CH_3).
19. The proton NMR spectrum of the metabolite changes upon storage for about one month. For example, the sharp doublet at 9.01 ppm disappears and two new signals are observed at 10.2 and 9.65 ppm. The latter signal is consistent with the chemical shift for the aldehyde proton in **28**, as determined by the chemical shift for the aldehyde

proton observed in the proton NMR spectrum from an authentic sample of the aldehyde.
20. An alternative explanation is that benzamide **22** is responsible for this activity; however, the K_i for this compound was determined to be 2.7 μM, about 100-fold less active than the synthetic sample of **23** and 3-fold less active than the parent compound **1**.
21. Hydroxybenzimidazole **6** could have been a viable candidate for development due to its increased potency relative to **1**; however, this option was not considered for two reasons. First of all, this class of inhibitors did not possess sufficient potency at pH 7.4 in physiological concentrations of free zinc. More importantly, we were unable to establish evidence for the formation of stable, inhibitory ternary complexes of zinc, tryptase, and **1** in the human mast cell granules (Amos Baruch and James Clark, unpublished work).